Cytometry
PART A
Journal of the International Society for Advancement of Cytometry

# Flat-Top Illumination Profile in an Epifluorescence Microscope by Dual Microlens Arrays

**Frank A. W. Coumans,[1]* Edwin van der Pol,[2] Leon W. M. M. Terstappen[1]**

[1]Department of Medical Cell BioPhysics, MIRA institute, University of Twente, Enschede, The Netherlands

[2]Biomedical Engineering and Physics, Laboratory Experimental Clinical Chemistry, Academic Medical Center, University of Amsterdam, Amsterdam, The Netherlands

Received 4 March 2011; Revision Received 10 January 2012; Accepted 7 February 2012

Grant sponsor: Veridex LLC, Raritan, NJ, USA.

Additional Supporting Information may be found in the online version of this article.

*Correspondence to: Frank Coumans, Medical Cell Biophysics Group, University of Twente, Carre, Room C4431, P.O. Box 217, 7500 AE Enschede, The Netherlands

Email: f.a.w.coumans@utwente.nl

Published online 5 March 2012 in Wiley Online Library (wileyonlinelibrary.com)

DOI: 10.1002/cyto.a.22029



## Abstract

Low uniformity in illumination across the image plane impairs the ability of a traditional epifluorescence microscope to quantify fluorescence intensities. Two microlens arrays (MLAs) were introduced into the illumination path of two different epifluorescence microscope systems to improve the uniformity of the illumination. Measurements of the uniformity of illumination were performed with a CCD camera in the focal plane and with fluorescent beads in the image plane. In semi critical alignment, a uniformity of illumination of 15–23% was found compared with 1–2% in the modified system. Coefficient of variation (CV) of fluorescent beads measured on the unmodified system was 20.4% ± 5.3% in semi critical alignment and 10.8% ± 1.3% in Koehler alignment. On the MLA systems, CV was 7.9% ± 2.0% and on a flow cytometer, the CV was 6.7% ± 0.7%. Implementation of MLAs in an epifluorescence microscope improves the uniformity of illumination, thereby reducing the variation in detection of fluorescent signals of the measured objects and becomes equivalent to that of flow cytometry. © 2012 International Society for Advancement of Cytometry

## Key terms

microlens array; coefficient of variation; epifluorescence microscopy; homogeneous illumination profile; beam shaping; flat top

In a traditional epifluorescence microscope, there is a tradeoff between the illumination uniformity and power. Koehler illumination is used to achieve high uniformity at the expense of illumination intensity, whereas semi-critical alignment is used to achieve high illumination intensity at the expense of uniformity (1). In Koehler illumination, the light source is focused onto the back pupil of the objective, while in semi-critical illumination, the light source is focused slightly beyond the sample. Poor uniformity results in large spatial intensity variations at the focal plane, while low illumination intensity requires longer illumination times and results in additional bleaching of the sample. With Koehler alignment, an improvement in CV can be obtained (2). If a better CV is needed, the signal can be corrected by shading correction (3,4) or by using the middle 50% of the image (5) to reduce the CV down to 3%. Multiplication is effective in cases where the illumination profile is well known and the signals are bright. In cases where the signal is dim, multiplication is not effective because signal to noise ratio is not changed. Reduction of the field of view increases the time needed for acquisition. A hardware solution that improves the CV without any of these disadvantages is desired. Previously, a double microlens array (MLA) was used to improve the uniformity of the illumination from a tungsten-halogen lamp (6) and from lasers (7). Here, we demonstrate that epifluorescence microscopes equipped with a mercury arc lamp can be retrofitted with a double MLA system to achieve the uniformity of Koehler alignment, while achieving the illumination intensity of semi-critical alignment. The need for such improvements arises from our desire to improve the sensitivity of detection of rare circulating tumor cells (CTC; 8) and the improvement for the quantification of treatment targets present at low densities on these CTCs such as IGF-1R and Her-2 (9–11).

ISAC
International Society for Advancement of Cytometry

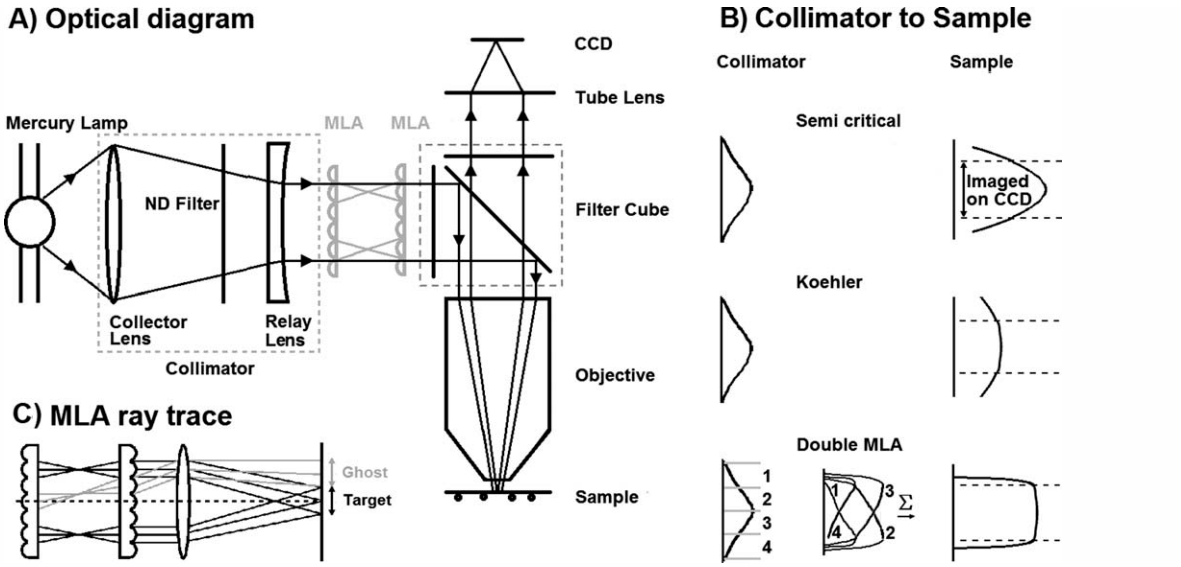


**Figure 1. A**: Optical diagram of the epifluorescence microscope with illumination and detection paths. Rays shown are for semi critical alignment. The collimator was optimized during modification of the microscope. Two MLA were inserted between the relay lens and the filter cube (gray). B: Cartoons illustrating the truncation of the illumination field in semi critical alignment Koehler alignment and in the MLA system. In the MLA system, the illumination field is split into pieces. Each piece is superimposed to yield a more uniform illumination. **C**: Ray trace for MLA system, black lines illustrate how the rays passing through different lenslets are superimposed, gray lines show how incoming light with too high an angle forms a ghost image next to the target.

## Materials and Methods

### Epifluorescence Microscope

Two epifluorescence microscopes were modified to test the implementation of a double MLA system. The first microscope is the CellTracks Analyzer II (Veridex LLC, Raritan, NJ). Figure 1A shows the optical diagram of the microscope. The illumination path contains a 100 W HBO lamp (USH-103D, Ushio, Cypress, CA), a collection lens (Quartz Epi-FL Collector Lens, Nikon, Tokyo, Japan) and a plano-concave relay lens (fused silica focal length −150 mm, Edmund optics, Barrington, NJ) to generate a collimated beam. Four custom designed filter cubes (blue: ex 365/20, em LP 400; green: ex 475/20, em 510/20; yellow: ex 547/12, em 578/25; red: ex 620/30, em 580/55; Corion, Franklin, MA) direct a selected wavelength band to a 10× NA 0.45 objective (CFI plan apochromat, Nikon, Tokyo, Japan). The emitted light is collected by the objective and passed through the filtercube to a tube lens with 200 mm focal length (Infinity tube lens unit for CFI, Nikon, Tokyo, Japan), which forms an image on a TE cooled CCD camera (1412AM, DVC, Austin, TX). In the focal plane, the area imaged is 0.90 × 0.67 mm and referred to as the pickup area. Figure 1B illustrates that truncation of the illumination field results in inhomogeneous illumination using the unmodified system.

The second system is the Eclipse 400 microscope system (Nikon, Tokyo, Japan) equipped with a C4742-95 CCD camera (Hamamatsu, Japan). The optical layout of the Eclipse is equivalent to the CellTracks Analyzer II. The same model 10× objective was used. The filter cubes had the same wavelength specifications, but were manufactured by Omega Optical (Brattleboro, VT). After measurements were performed with Koehler alignment the microscope was modified for measurements with the MLA system modification. Figure 1C illustrates that the intensity of the illumination is reduced with Koehler alignment.

### Double Microlens Array

If the light bundle from the collimator is uniformly distributed, the illumination on the sample can be uniform. Typically, the bundle from the illuminator is not uniform, but the nonuniformity is symmetrical around the optical axis. This symmetry is used to achieve uniform illumination with an MLA pair. Two MLAs were introduced in the system as illustrated in Figure 1A. A MLA contains an array of lenslets, which split the incoming bundle into segments and can be used to produce homogeneous illumination. Each segment is imaged onto the focal plane, superimposed on top of each other as illustrated in Figures 1B and 1C. The nonflatness of a segment of the incoming bundle is cancelled out by a segment on the opposite side of the optical axis. This results in a "flat top" illumination profile with sloped sides. Using two MLAs in sequence, this slope becomes very steep, reducing the power lost outside the pickup area. The ideal size of the flat top generated by a double MLA is slightly larger than the size of the pickup area to achieve high uniformity while maintaining the majority of illumination power inside the pickup area. The size of the flat top can be calculated with Eq. (1; 12):

$$Y = \frac{p_L f_F}{f_{L1} f_{L2}} (f_{L1} + f_{L2} - s) \quad (1)$$

With $Y$, the flat top cross section, $p_L$ the pitch of the MLA, $f_F$ the focal length of the objective, $f_{L1}$ and $f_{L2}$ the focal length of the first and second MLA, respectively, and $s$ the distance

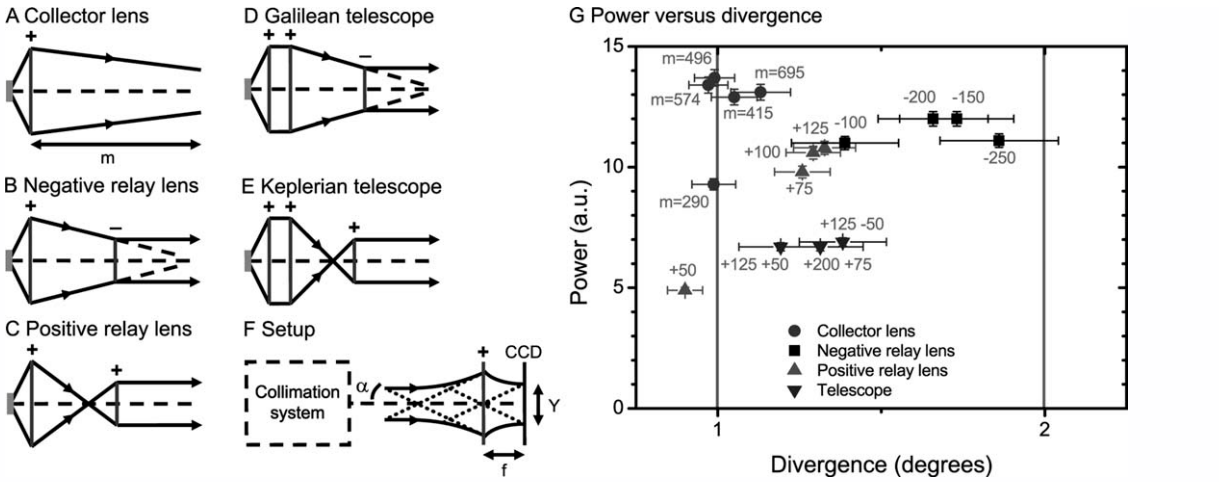


**Figure 2.** Collimator designs consisting of (**A**) a collector lens only, (**B**) a negative relay lens, (**C**) a positive relay lens, (**D**) a Galilean telescope, and (**E**) a Keplerian telescope. **F**: A CCD camera was placed in the focal plane *Y* of a positive lens with focal distance *f* to measure the divergence $\alpha$ and transmission power of each collimator. **G**: Power versus normalized mean divergence for various collimators. For the collector lens collimators, the gray labels indicate the distance *m*. For the other collimators, the lens focal lengths are shown. The solid vertical lines indicate the specified maximum input divergence of two commercially available MLAs. The collector lens collimators have the highest power and the lowest divergence but require a large path length. Negative relay lens collimators perform well on power versus divergence while maintaining a compact system.

between the two MLAs. With different pitches for *x* and *y* direction, a rectangular flat top is created. CC-Q-1015S and CC-Q-300S are the commercially available MLAs that match the pickup area closest and are made of UV transmitting quartz (SUSS Microoptics, Neuchâtel, Switzerland). The maximum input divergence of these two MLAs is 2° and 4°, respectively.

### Collimator Design

For the introduction of a double MLA in the system, the lenslets of both MLAs need to be aligned. Light that passes through the double MLA at an angle through nonaligned lenslets will generate ghost images next to the pickup area, see Figure 1C. This limits the divergence that the MLA can handle. Various collimators consisting of the collector lens and the relay lens were tested for their power transmission and forward divergence. The collimators that were tested are illustrated in Figure 2A–E and include a single positive lens, a single negative lens, and a Galilean and Keplerian telescope. All lenses used were 25 mm diameter fused silica plano-concave or plano-convex lenses (Edmund Optics, Barrington, NJ) with focal lengths as shown in Figure 2G. The forward divergence and power transmission of each collimator were measured by imaging the output of the collimator through a single lens with focal length $f = 100$ mm (50 mm diameter fused silica plano-concave lens, Edmund Optics, Barrington, NJ) onto a CCD camera (1412AM, DVC, Austin, TX), see Figure 2F. At the focal plane, the divergence $\alpha$ is related to the full width at half maximum of the bundle diameter *Y* by Eq. (2; 13):

$$\alpha = \frac{Y}{2f} \tag{2}$$

The divergence for two perpendicular directions in the focal plane was determined, averaged, and normalized to the beam size as reduction in beam size increases the divergence linearly. Due to the size of the MLA, each collimator was aligned to achieve a full width at half maximum of $<10 \times 10$ mm. The sum of the power on the CCD was taken as the transmitted power.

### Calculations

To investigate the impact of each design parameter on the illumination in the focal plane, the Fraunhofer approximation of the scalar Fresnel-Kirchhoff diffraction theory is applied to calculate the one-dimensional intensity distribution at the focal plane of the microscope objective as described elsewhere (14). Our calculations are done in Matlab 2007b (Mathworks, Natick, MA). For reference, a summary of the model components is given in Supporting Information S1, and the Matlab m-file in Supporting Information S2. Parameters used are based on the CC-Q-300S MLA and the Nikon 10× NA 0.45 objective.

### Measurement of Illumination Quality

Collimators were implemented in the microscope together with the optimal MLA pair. The impact of this modification was determined on the same system before and after modification was complete for the four filter cubes. To determine the illumination quality, the intensity distribution was measured by placing a CCD camera (Deep sky imager II, monochrome CCD board version camera, Meade Instruments, Irvine, CA) in the focal plane of the objective. The pickup area covers only 8% of the CCD area; therefore, the obtained image can be used to measure the fraction $\eta$ of the total transmitted light that hits the pickup area (Eq. 3) as well as the coefficient of variation (CV) of illumination

within the pickup area (Eq. 4). $\sum I_{\text{pixel}}$ is the sum of intensities for all pixels.

$$\eta = \frac{\sum_{\text{Pickup}} I_{\text{Pixel}}}{\sum_{\text{CCD}} I_{\text{Pixel}}} 100\% \quad (3)$$

$$\text{CV} = \frac{\text{SD}_{\text{Pickup}}}{Mean_{Pickup}} 100\% \quad (4)$$

Because the CCD camera did not fit in the Eclipse 400, measurements of the illumination quality were performed only in the CellTracks II.

### Measurement of CV Using Fluorescent Beads

Broad-spectrum fluorescent magnetic beads (UMC4F COMPEL beads, Bangs Laboratories, Fishers, IN) with diameter 8 $\mu$m were chosen in order to use the same sample cartridge used for the routine analysis of clinical samples in the microscope system. The sample cartridge is filled with beads and distributed equally over the analysis surface by means of the specific configuration of the magnets surrounding the chamber (8,15). Images were acquired to cover the analysis surface for each of the four fluorescent filter cubes and were analyzed in Matlab 2007b (Mathworks, Natick, MA). In short, thresholds were set on the images at a level of three times the CCD readout noise, objects with sizes more than 20% over or under 8-$\mu$m diameter were excluded and the peak intensity of the remaining objects was determined. The bead cartridge was scanned on the unmodified CellTracks in semi critical alignment, the unmodified Eclipse 400 in Koehler alignment, and both microscopes equipped with the MLA systems.

In addition, the beads were scanned on a flow cytometer (FACSCalibur, BD Biosciences, San Jose, CA) setup according to published guidelines (16). Due to absence of a UV laser, beads were measured only in the green (FL1 488-530/30), yellow (FL2 488-585/42), and red (FL4 635-661/16) channel. Samples were run at a low flow rate (LO). Acquisition gate was set on forward scatter, minimum 15 (beads = 150).

No compensation was applied and CV and mean intensity were determined using FCS Express 4 (De Novo Software, Los Angeles, CA). Gates were set around the peak intensity to exclude doublets. Histograms were created for all data and means and CV calculated. Since the detection method differs substantially, the data from the flow cytometer was multiplied by a correction factor to make the mean intensity value fall on the mean of the value measured on the two microscope systems.

## Results

### Collimator Design

Figure 2G shows the results of power and divergence measurements for different collimators. The different collimator designs are shown in annotations next to each data point. Highest power transmission with lowest divergence is achieved by the collector lens focused near infinity. The total path length was varied as needed to achieve best performance. Collimators consisting of just the collector lens were the only ones, which had high power transmission and a forward divergence not exceeding the maximum for the CC-Q-1015S MLA. With these collimators, the path length from lens to first MLA will be very long (40–70 cm), which exceeds the size that fits within the microscope enclosure. The telescopes performed poorest on power transmission, possibly due to the 25 mm lens diameter used. The negative relay lens designs had good power transmission, did not exceed the maximum input divergence for the CC-Q-300S MLA and were the most compact collimators. The positive relay lens systems had lower forward divergence, but also lower power transmission and required more space than the negative relay lenses. The −150 mm lens is the most compact and has the highest power, while not exceeding the maximum forward divergence of the CC-Q-300S MLA. This collimator was therefore selected for the MLA system and implemented in the microscopes.

### MLA Simulations

The calculation parameters are $\alpha_{\max} = 1.7^\circ$, $f_F = 20$ mm, $f_L = 4.75$ mm, $N_0 = 32$, $p_L = 0.3$ mm, where $\alpha_{\max}$ is the divergence, $f_F$ is the focal length of the objective, $f_L$ is the focal length of the lenslets of the MLA, $N_0$ is the number of lenslets, and $p_L$ is the pitch of the lenslets. The spectral distribution of the mercury arc lamp was measured (not shown) and included in the model. Figure 3A shows the calculated 1D illumination profile for the microscope containing a single MLA. The illumination profile within the pickup area is homogeneous, but the power efficiency of 8.3% is rather low. Figure 3B shows the calculated illumination profile after addition of the second MLA. The distance $s$ between the two MLAs is equal to $f_L$, resulting in a wide flat top with steep edges and a power efficiency of 37.3%. By increasing $s$ the flat top becomes smaller, with less steep edges. Figure 3C shows the calculated illumination profile for two MLAs separated by a distance $s$ equal to 1.5 times $f_L$. Now, the power efficiency is 64.8% at the expense of homogeneity, since the edges of the flat top also fall within the pickup area.

### Measurement of the Illumination Quality

The results of the measurement of the CV under the objective are shown in Figure 4 and Table 1. Figure 4 shows the illumination intensity distribution of the CellTracks system before and after modification. Table 1 shows the illumination efficiency $\eta$ and the CV within the pickup area for all channels. In the unmodified microscope, CVs of 15–23% are measured, while in the MLA modified microscope they are 1.2–1.5%. The illumination efficiency is slightly better for the MLA modified microscope (38–43%) compared with the same microscope before modification (28–40%).

### Measurement of CV Using Magnetic Fluorescent Beads

Figure 5 shows an image of fluorescent beads with the Nikon in Koehler, semi-critical alignment and with the MLA modification. Figure 6 shows histograms for the beads

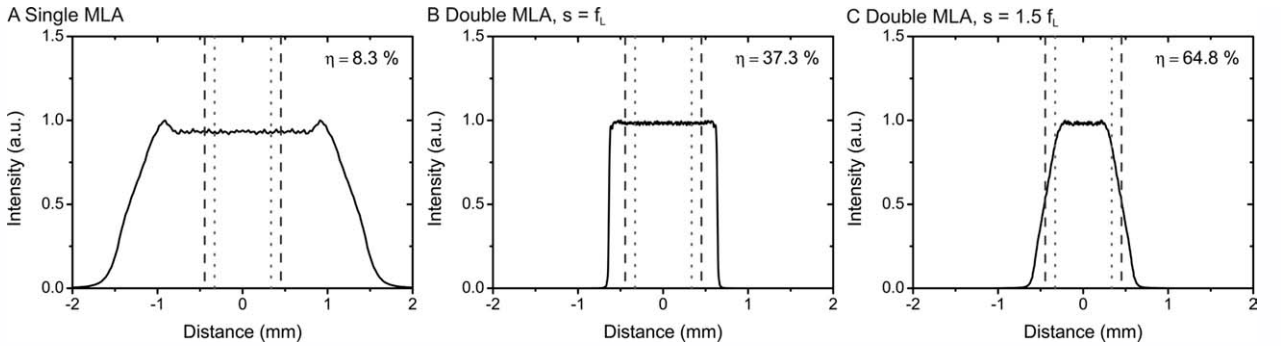


**Figure 3.** Calculated 1D illumination profile for the epifluorescence microscope containing (**A**) a single MLA, (**B**) two MLAs separated by a distance *s* equal to the focal length of the lenslets $f_L$, and (**C**) two MLAs separated by a distance *s* equal to 1.5 times $f_L$. The dashed and dotted lines indicate the pickup area, which is given by the width at the focal plane of both directions that is imaged on the CCD chip. The power efficiency $\eta$ is the ratio between the power at the pickup area and the total power. A: The illumination profile of the pickup area for a microscope containing a single MLA is homogeneous, but the power efficiency is low. B: By adding a second MLA at distance $s = f_L$ the illumination profile remains homogeneous and the power efficiency increases 4.5-fold. C: By increasing the distance "*s*" to 1.5 $f_L$ the power efficiency increases another 1.7-fold at the expense of homogeneity.

measured with the four fluorescence cubes. The histograms show that the CV of the MLA CellTracks system is much improved compared with the CV measured on the unmodified CellTracks. The intensity on the MLA system is higher than semi-critically aligned microscope by 20–160%. The CV on the MLA Eclipse 400 is slightly improved and the signal level is 2–4 folds higher when compared to a Koehler aligned Eclipse 400. The CV measured on the flow cytometer equipped with a 488 and 633 nm laser was similar to the CV found with the MLA systems.

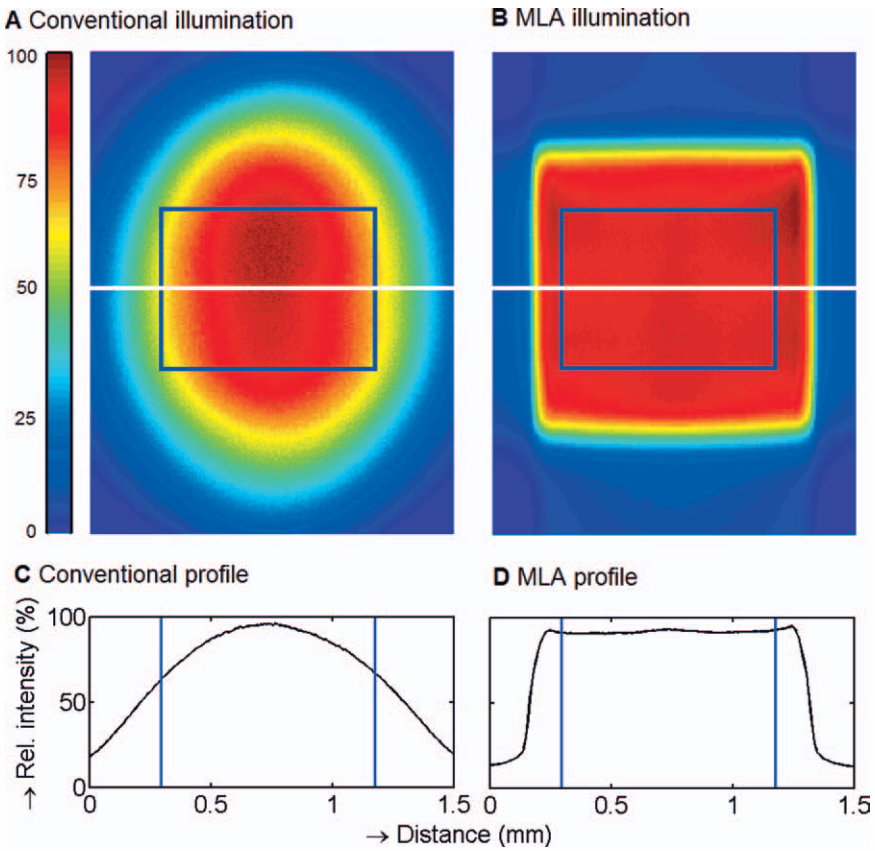


**Figure 4.** Normalized illumination profile of (**A**) the conventional microscope and (**B**) the modified microscope containing two MLAs. The solid blue lines mark the pickup area, which is the area that is imaged by the CCD of the microscope. The white horizontal line indicates the position where a cross section of the illumination profile of (**C**) the conventional microscope and (**D**) the modified microscope was taken. The illumination profile of the same microscope before and after modification shows a large improvement in homogeneity.

**Table 1.** Illumination efficiency ($\eta$, %) and CV (%) measurements on the microscope system before (EPI) and after modification (MLA)

| | EPI | | MLA | |
|---|---|---|---|---|
| | $\eta$ | CV | $\eta$ | CV |
| DAPI | 28 | 14.8 | 38 | 1.4 |
| FITC | 34 | 18.4 | 41 | 1.5 |
| PE | 36 | 18.4 | 42 | 1.2 |
| APC | 40 | 23.1 | 43 | 1.3 |

## Discussion

A double MLA is introduced in an epifluorescence microscope to improve the homogeneity of the illumination resulting in an improvement in the sensitivity and quantification of fluorescent signals. Automated image analysis algorithms for detection of fluorescently labeled cells can greatly benefit from such improvement as they apply a threshold on the measured fluorescence intensity to discriminate between the labeled and nonlabeled cells in the sample. The efficacy of thresholding strongly depends on the homogeneity of the illumination as inhomogeneous illumination will result in a variation of the detection limit across the image and impairs reliable quantification. An application in need for such improvement is the identification of fluorescently labeled CTC in images acquired by fluorescent microscopy in for example the CellSearch system (8). In this system CTC candidates are identified as objects that express cytokeratin labeled phycoerythrin (CK-PE). The efficiency of detection of cells with relatively low CK-PE signals will thus vary across the image and can greatly benefit from a homogeneous illumination. For assessment of treatment targets on these tumor cells, low intensity expression will result in some cells being missed, pending on the illumination of the specific area and quantification will be hampered by the lack of uniformity.

A variety of approaches can be applied to improve the homogeneity of the illumination of epifluorescence microscopes such as the use of aspheric lenses and mirrors (17), diffractive optics (18), ND filters (19), and engineered diffusers (20). Aspheric lenses and mirrors perform well with Gaussian beams, but the mercury arc lamp does not produce a Gaussian beam. Diffractive optical elements are designed for a specific wavelength, which makes them unsuitable for use in an application where four different illumination bands are used. ND filters can achieve excellent uniformity, but the cost is an order of magnitude reduction in light intensity, making them unsuitable for a low light level application. If custom dimensioned for application in this system, engineered diffusers are expected to be similar in performance to the MLAs presented. Available standard versions would however result in too much loss of power and a custom design was too costly to implement. In addition, the images from a Koehlered microscope could be corrected in a postprocessing step if the illumination profile is known. Such a procedure reduces spatial dependence of signal level, but does not improve signal to noise ratio, which is most important when dealing with dim signals.

Implementation of double MLA in an epifluorescence microscope improves the uniformity of illumination without sacrificing illumination intensity when compared with semi critical alignment and improves illumination intensity without sacrifice to illumination uniformity when compared with Koehler alignment. Implementing the MLA system is relatively simple and cost effective. In Supporting Information S3, we describe how other epifluorescence microscopes can be modified and aligned. In contrast to Koehler alignment, the alignment of the MLA system is stable and does not need frequent optimization. The only alignment that may be needed is that of the lamp after bulb replacement. Because the size of the field of view is matched to the CCD camera the use of binoculars on the same system would result in a smaller field of view and additional modifications would be needed when this is not desired. The distance between the last MLA and back focal plane of the objective needs to be $<$100 mm to achieve optimal performance. To achieve this, we had to remove the objective turret in the Eclipse 400. A sufficiently compact objective turret is possible, but not available from Nikon at this time. This distance limitation could be mitigated by making the system telecentric, but doing so would require much larger MLA and thus a more extensive modification of our microscopes.

Several collimator designs were tested. A single collection lens without further optics performed best with respect to power and forward divergence, but required too much length

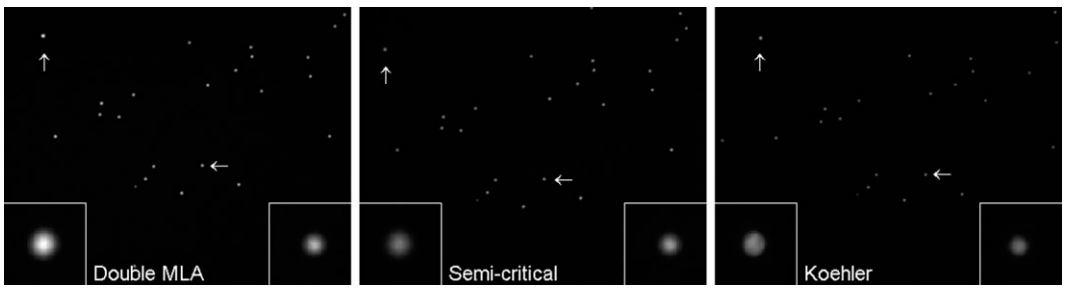


**Figure 5.** Image of beads under epifluorescence microscope in MLA alignment, semi critical, and Koehler alignment. Arrows point to the enlargements in the corners of the screen. The bead in the middle (horizontal arrow, enlargement on right) is equally bright on both MLA and semi critical system, but dimmer on the Koehler system. The bead in the corner (vertical arrow enlargement on left), is brightest on the MLA, and dimmer on both semi critical (low illumination intensity in corners) and Koehler system (uniform illumination with lower overall intensity).

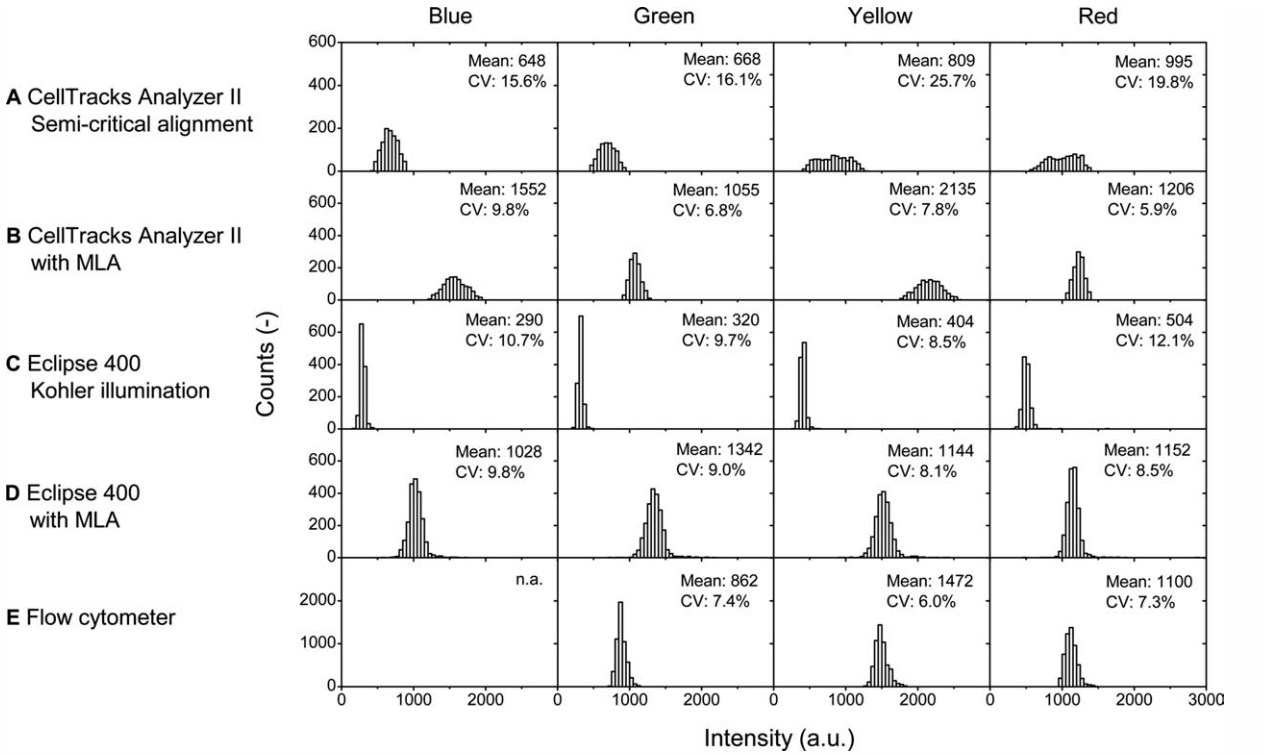


**Figure 6.** Intensity distributions of beads measured by the semi critically aligned CellTracks microscope (**A**), the Koehler aligned Eclipse 400 (**B**), the modified Eclipse 400 containing 2 MLAs (**C**), the modified CellTracks (**D**), and a flow cytometer (**E**). Measurements on the microscopes were performed with filter cubes with blue, green, yellow, and red emission. The flow cytometer measurements were performed with 488 nm laser line excitation and filters tuned for yellow and green detection and the 633 nm laser line with filters for red detection. No measurement was available for the UV/blue region because the flow cytometer lacked a UV laser. The intensity distributions obtained by the flow cytometer are scaled on the mean intensities obtained on the conventional and modified microscopes.

to make application practical in the microscope. We did implement a negative relay lens collimator, which achieved similar power with a small increase in forward divergence. The differences in the power transmission and divergence with the various collimator designs may be partially explained by a different distance between arc lamp and the collector lens, changing the effective NA of the collector lens.

The 100 W HBO lamp has an arc with a high power density, making it relatively easy to collimate and achieve low divergence angle. Higher power lamps tend to have larger arcs, which are harder to collimate. Selection of an MLA pair with a higher maximum divergence angle may allow for creation of a flat top with a higher power light source, and thus allow higher brightness on the sample.

Modeling shows that the size of the flat top can be tuned by changing the inter MLA distance, allowing compensation of a mismatch between CCD and MLA dimensions at the cost of some illumination power. We measured an illumination CV of 1.2–1.5% and an efficiency of 38–43% using a camera underneath the objective, which matched our theoretical model quite well. We estimate a further 25% increase in illumination intensity could be gained by custom designing an MLA array to match the CCD camera.

We did not measure the same low CV using beads in normal imaging mode. In both microscope systems, the MLA modified microscope outperformed the unmodified microscope. The MLA modified CellTracks performed better than the MLA modified Nikon Eclipse. This difference may be attributed to two factors; first, the Nikon body design limits dimensions between the different components of the illumination path and second, mechanical modifications may not have been sufficiently precise for best results. The CV measured on the flow cytometer was similar to the CV measured on the MLA modified microscope, which makes it likely that the measured CV can mainly be contributed to the CV of the beads. An exact comparison of flow cytometry to the MLA imaging system is not possible because the exclusion of doublets and noise are handled differently due to hardware differences. Even though the signal intensity was higher on the MLA system compared with the conventional system, comparisons are difficult because the intensities between different microscopes can vary by up to two fold.

Implementation of MLAs in epifluorescence microscopes is uncomplicated, inexpensive, and can improve the detection of cells with low antigen expression, as it no longer depends on the position of a cell in the image. In addition, smaller differences in antigen expression between different cells can be detected, which improves the quantification of antigen expression.

## Acknowledgments

The authors acknowledge Jan Key for performing flow cytometry on the beads. LWMM is a consultant for Veridec LLC.

## Literature Cited

1. Florijn RJ, Bonnet J, Vrolijk H, Raap AK, Tanke HJ. Effect of chromatic errors in microscopy on the visualisation of multi-color fluorescence in situ hybridization. Cytometry 1996;23:8–14.
2. Wang N, Pan Y, Heiden T, Tribukait B. Fluorescence image cytometry for measurement of nuclear DNA content in surgical pathology. Cytometry 1995;22:323–329.
3. Model MA, Burkhardt JK. A standard for calibration and shading correction of a fluorescence microscope. Cytometry 2001;44:309–316.
4. Klein AD, van den Doel R, Young IT, Ellenberger SL, van Vliet LJ. Quantitative evaluation and comparison of light microscopes. In: Farkas DL, Leif RC, Tromberg BJ, editors.Optical Investigation of Cells In Vitro and In Vivo. Proc SPIE. Prog Biomed Opt 1998;3260:162–173.
5. Bright GR, Fisher GW, Rogowska J, Taylor DL. Fluorescence ratio imaging microscopy: Temporal and spatial measurements of cytoplasmic pH. J Cell Biol 1987;104:1019–1033.
6. Ji JK, Kwon YS. Conical microlens arrays that flatten optical-irradiance profiles of nonuniform sources. Appl Opt 1995;34:2841–2843.
7. Scholtens TM, Schreuder F, Ligthart ST, Swennenhuis J, Tibbe AGT, Greve J, Terstappen LWMM. Cell tracks TDI: An image cytometer for cell characterization. Cytometry A 2011;79A:203–213.
8. Allard WJ, Matera J, Miller MC, Repollet M, Connelly MC, Rao C, Tibbe A, Uhr JW, Terstappen LWMM. Tumor cells circulate in the peripheral blood of all major carcinomas but not in healthy subjects or patients with non-malignant diseases. Clin Cancer Res 2004;10:6897–6904.
9. de Bono JS, Attard G, Adjei A, Pollak MN, Fong PC, Haluska P, Roberts L, Melvin C, Repollet M, Chianese D, et al. Potential applications for circulating tumor cells expressing the insulin growth factor-I receptor. Clin Cancer Res 2007;13:3611–3616.
10. Riethdorf S, Müller V, Zhang L, Loibl S, Komor M, Roller M, Huober J, Fehm T, Schrader I, Hilfrich J, Holms F, Tesch H, Eidtmann H, Untch M, von Minckwitz G, Pantel K. Detection and HER2 expression of circulating tumor cells: Prospective monitoring in breast cancer patients treated in the neoadjuvant geparquattro trial. Clin Cancer Res 2010;16:2634–2645.
11. van der Pol E, Hoekstra AG, Sturk A, Otto C, van Leeuwen TG, Nieuwland R. Optical and non-optical methods for detection and characterisation of microparticles and exosomes. J Thromb Haemostasis 2010;8:2596–2607.
12. Voelkel R, Weible KJ. Laser beam homogenizing: Limitations and constraints. In: Duparré A, Geyl R, editors.SPIE Conference proceedings vol 2008; 7102. Bellingham, WA: SPIE Publications; Abstract71020J.
13. Wright D, Greve P, Fleischer J, Austin L. Laser beam width, divergence and beam propagation factor: An international standardization approach. Opt Quantum Electron 1992;24:S993–S1000.
14. Büttner A, Zeitner UD. Wave optical analysis of light emitting diode beam shaping using micro lens arrays. Opt Eng 2002;41:2393–2401.
15. Tibbe AGJ, de Grooth BG, Greve J, Dolan GJ, Rao C, Terstappen LWMM. Magnetic field design for selecting and aligning immunomagnetic labeled cells. Cytometry 2002;47:163–172.
16. Maecker HT, Trotter J. Flow cytometry controls, instrument setup and the determination of positivity. Cytometry Part A 2006;69A:1037–1042.
17. Hoffnagle JA, Jefferson CM. Design and performance of a refractive optical system that converts a Gaussian to a flattop beam. Appl Opt 2000;39:5488–5499.
18. Nemoto K, Fujii T, Goto N, Takino H, Kobayashi T, Shibata N, Yamamura K, Mori Y. Laser beam intensity profile transformation with a fabricated mirror. Appl Opt 1997;36:551–557.
19. Chang SP, Kuo JM, Lee YP, Lu CM, Ling KJ. Transformation of Gaussian to coherent uniform beams by inverse-Gaussian transmittive filters. Appl Opt 1998;37:747–752.
20. Sales TRM. Structured microlens arrays for beam shaping. Opt Eng 2003;42:3084–3085.